

Direct observation of domain walls in NiFe films using high-resolution Lorentz microscopy

Bunsen Y. Wong and David E. Laughlin

Department of Materials Science and Engineering, Carnegie Mellon University, Pittsburgh, Pennsylvania 15213

A novel approach to observe the interaction between magnetic domain wall and nanoscale microstructural features is demonstrated. The method is based on Focault mode Lorentz microscopy and utilizes a Gatan energy image filter to provide additional magnification. A postexperimental image processing technique was applied to separate lattice diffraction from that induced by magnetic domains. The effect of NiFe thickness on the width of a 180° Néel wall has been studied. It was found that the thickness dependence has a similar profile to the theoretically predicted trend but the actual wall thickness is smaller than the calculated values. © 1996 American Institute of Physics. [S0021-8979(96)57308-6]

I. INTRODUCTION

Magnetic properties of materials are closely associated with the magnetic domain configurations and the interaction between domain walls and microstructural features. Techniques such as Lorentz microscopy in both the conventional and scanning transmission mode,^{1,2} spin polarized scanning electron microscopy,³ and magnetic force microscopy^{4,5} have been developed to address these issues. However, these techniques are unable to resolve the microstructure-domain interactions on a nanoscale such as those in thin films. In this work, we report on a novel technique utilizing a Gatan energy image filter (GIF) and based on Focault mode Lorentz microscopy which can resolve both fine magnetic domains and microstructural features. A schematic of the GIF unit attached to the transmission electron microscope (TEM) is shown in Fig. 1. In the present study, the function of the GIF is twofold as follows.

(1) Conventional Lorentz microscopy requires a field-free objective lens which generally limits the image magnification to $3000\times$. The magnetic magnifying lenses ($\times 18.75$) and the charge-coupled-device (CCD) camera ($\sim \times 8$) contain within the GIF can provide additional magnification power which helps achieve a theoretical resolution of 1 nm in this technique.

(2) The elastically scattered electrons which have undergone magnetic phase change can be separated from the inelastically scattered electrons by using the energy filter slit. Hence, a higher signal-to-noise ratio in the magnetic image can be obtained. We have applied this technique to study the effect of film thickness on the 180° domain-wall width in sputter-deposited NiFe thin films in order to demonstrate the capacity of this new technique.

II. EXPERIMENTAL PROCEDURES

$\text{Ni}_{81}\text{Fe}_{19}$ films of thicknesses ranging from 7 to 35 nm were deposited on NaCl substrates by rf diode sputtering. The Ar sputtering gas pressure was 5 mTorr and a forward power of 50 W was used. The films were then floated off the substrates onto 3 mm Cu TEM grids. The domain-wall profiles and domain structures were studied using Focault mode Lorentz microscopy inside a JEOL 4000EX microscope op-

erating at 400 kV and attached to a GIF unit. Images were recorded with a CCD camera. Postexperimental image analysis was carried out with the interactive data language (IDL) image processing software so that the interference between magnetic and crystalline diffraction contrast can be minimized and an acute domain-wall profile can be determined.

III. RESULTS AND DISCUSSION

The magnetic domain contrast of two antiparallel domains in a 28-nm-thick NiFe film are shown in Figs. 2(a) and 2(b) along with the corresponding bright-field (BF) image in Fig. 2(c). The location of two reference grains is marked by arrows in the respective images. The average grain size of the lattice diffraction contrast can be clearly observed in the BF image which enables one to discern the grain morphology and other microstructural features. Hence, any interaction between domain boundaries and fine microstructural features can be easily made.

In the Focault mode, the displaced aperture intercepts one of the magnetically diffracted beams and results in black and white contrast within the TEM image. This variation in intensity outlines the local magnetization. In between the magnetic domains, a continuous gray contrast which represents the extent of the domain wall can be observed. In order

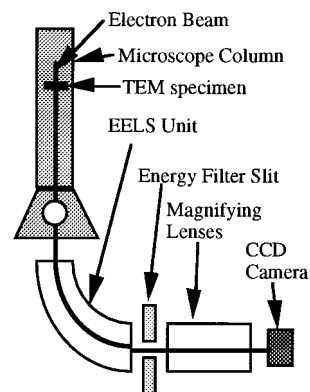


FIG. 1. A schematic of the GIF unit in relation to the TEM.

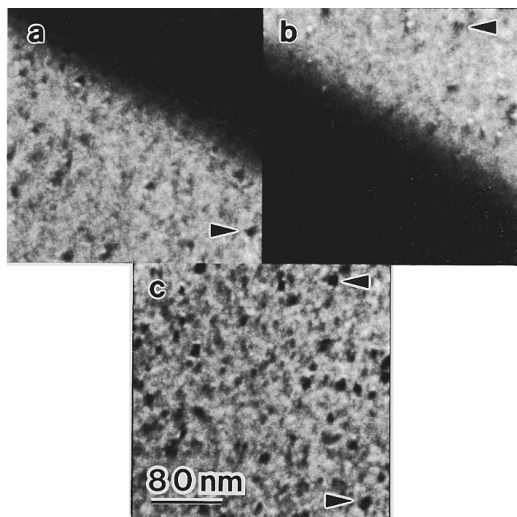


FIG. 2. (a),(b) Lorentz images of antiparallel domains in a 28-nm-thick thin film. (c) Corresponding BF image.

to determine the width of the 180° Néel wall, an integrated intensity profile across the image and perpendicular to the domain wall was obtained and the result is plotted in Fig. 3. This profile consists of three linear regimes and is an indirect representation of the magnetization direction within the image. The wall width is determined by the intercepts of the three linear regions as shown in Fig. 3. Similar Lorentz images for a 90° Néel wall in the same specimen are depicted in Fig. 4 and reference grains are marked with respect to the BF image. The gray regions in each frame represent domains which have half of their magnetization component blocked by the aperture whereas the origin of the black and white domains is similar to that explained above.

The Lorentz images that have been shown so far consist of diffraction contrast of both crystalline, i.e., granular, and magnetic nature. Hence, to assess the most appropriate profile of the domain wall, it is necessary to reduce the contribution from lattice diffraction within the image to a minimum. This is achieved through a postexperimental image processing technique and the path taken is illustrated in Fig. 5. In Figs. 5(a) and 5(b), an as-exposed Lorentz image is accompanied by its BF image, respectively. A negative or inverse of the BF image is shown in Fig. 5(c). In order to curtail the effect of lattice diffraction, intensity from the BF

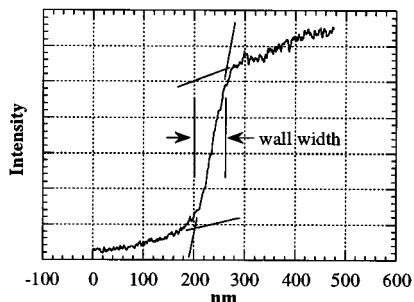


FIG. 3. Intensity trace across the 180° domain wall in 28 nm NiFe film.

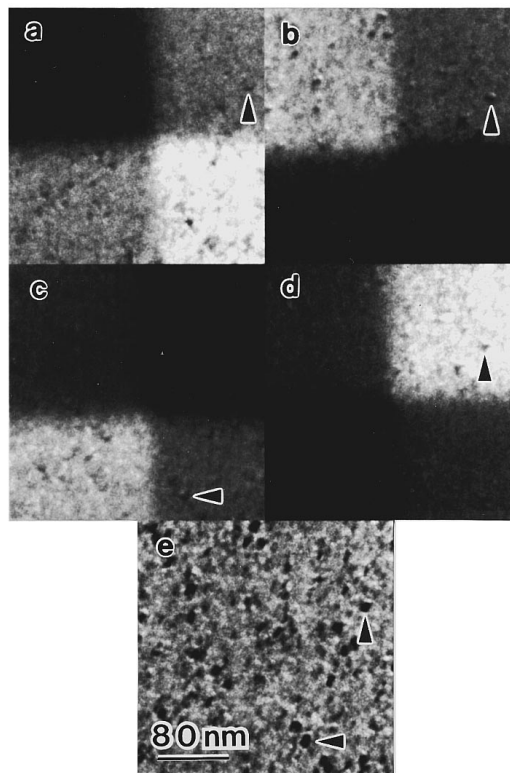


FIG. 4. (a)–(d) Lorentz images of 90° domains in a 28-nm-thick NiFe thin film with different components of the aperture blocked. (e) Corresponding BF image.

negative is added to the Lorentz image to achieve a more uniform contrast and the final processed image is shown in Fig. 5(d). The lattice diffraction within the white domain is reduced but not completely eliminated; however, the contrast in the black domain has deteriorated modestly after the image processing. The intensity profiles across the 180° Néel wall for the as-exposed and processed images are shown in

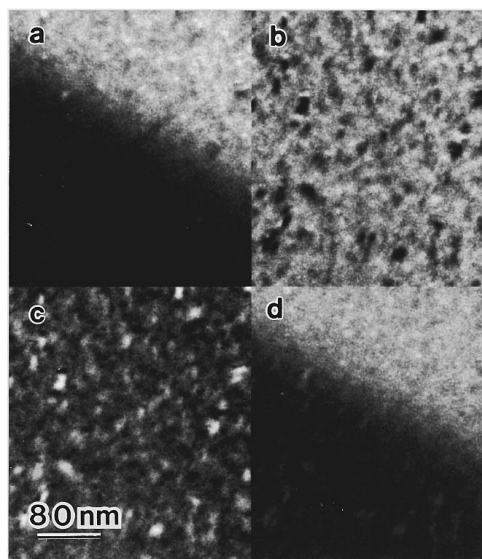


FIG. 5. (a) Lorentz images of a 28-nm-thick NiFe thin film. (b) Corresponding BF image. (c) Inverse of BF in (b). (d) Processed Lorentz image of (a).

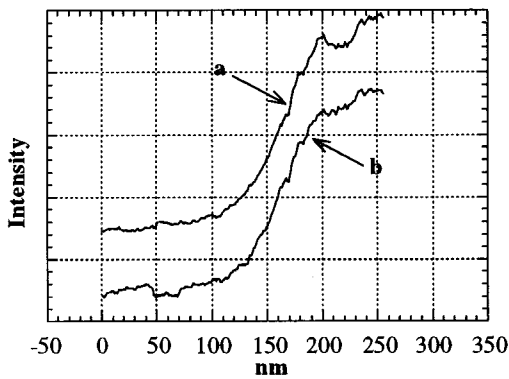


FIG. 6. Intensity profile across a 180° domain wall in a 28-nm-thick NiFe film: (a) as exposed and (b) processed images.

Fig. 6. The reduction in the intensity variation within the white domain has led to a better definition of the domain-wall width. By combining the two profiles, the 180° Néel wall width in NiFe films of various thicknesses has been measured and the results are plotted in Fig. 7. The dependence of wall width on film thickness is similar to the theoretical profile⁶ but the actual measured values are smaller than the calculated ones. They do, however, agree with other experimental observed values.⁷

IV. CONCLUSIONS

The dependence of 180° Néel wall width on the thickness of NiFe films has been measured by high-resolution Foucault mode Lorentz microscopy. This new technique incorporates the magnification capacity of the GIF unit and has

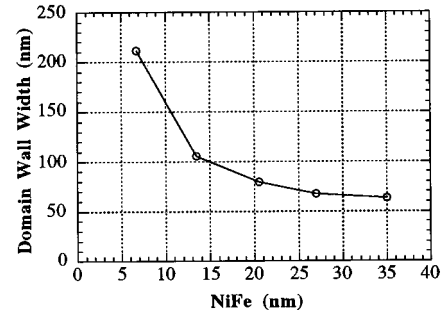


FIG. 7. Plot of 180° NiFe domain-wall width vs film thickness.

been demonstrated to achieve image resolution in the nanometer range. In addition, the lattice diffraction contrast can be reduced by applying postexperimental image processing technique which resulted in better magnetic contrast and a more accurate domain-wall profile.

ACKNOWLEDGMENTS

This work was supported by a grant from Hitachi Metals Ltd. The authors would like to thank Elke Fahrman and Dr. Marc DeGraef for their helpful discussions on image processing techniques.

¹H. W. Fuller and M. E. Hale, *J. Appl. Phys.* **31**, 238 (1960).

²J. N. Chapman and G. R. Morrison, *J. Magn. Magn. Mater.* **35**, 254 (1983).

³J. Unguris, G. G. Hmebree, R. J. Celotta, and D. T. Pierce, *J. Microsc.* **139**, SRP1-2 (1985).

⁴Y. Martin, *Appl. Phys. Lett.* **52**, 244 (1988).

⁵H. J. Mamin, *Appl. Phys. Lett.* **53**, 1563 (1988).

⁶T. Suzuki and C. H. Wilts, *J. Appl. Phys.* **40**, 1216 (1969).

⁷S. McVitie and N. J. Chapman, *J. Magn. Magn. Mater.* **83**, 97 (1990).